Bend in elastic lumped line and its effect on vibration pattern

S.B. Karavashkin and O.N. Karavashkina
Special Laboratory for Fundamental Elaboration SELF
187 apt., 38 bldg., Prospect Gagarina, Kharkov 61140, Ukraine
Phone: +38 (0572) 276624; e-mail: selflab@go.com , selflab@mail.ru

Website of Laboratory SELF: http://angelfire.lycos.com/la3/SELFlab
Website of the electronic journal SELF Transactions: http://angelfire.lycos.com/la3/selftrans

March 02, 2002

This paper is one of a large cycle of papers on obtaining the exact analytical solutions for vibrant elastic systems. This was published first in the electronic journal of laboratory SELF "SELF Transactions", vol.2, issue 1. Visiting this journal for free at http://angelfire.lycos.com/la3/selftrans you will find many other important results both on this subject and on many applications of this new method, as well as on many other subjects of mathematical physics and related themes. You will also find there that we check our results experimentally and yield the full coincidence of the calculation and experimental curves. And the main, this method gives exact solutions, and this is non-matrix. Already now we have solved many practically important problems which cannot be even approached properly by conventional methods. This is the future of dynamics out of which any development in any area of basic or applied wave physics is impossible.

You are welcomed to possess this wealth and contact us for discussions and joint further development.

Abstract

We prove that the bend in an elastic line does not effect on the solution pattern only, if the longitudinal and transversal stiffnesses of a line were equal. Basing on the proved theorem, we consider some models typical for the applications, particularly, models of a semi-finite elastic bended line, a homogeneous closed-loop elastic line and an elastic line having inequal longitudinal and transversal stiffness coefficients. We show that in the lines obeying the theorem conditions, with the remaining general solution, the vibration processes features are conditioned by the regularities of the co-ordinate system transformation. In case of inequal stiffness coefficients in the bend region, the complex dynamical thrusts and vibration break-downs take place, and the vibration amplitude grows. In the bend region the resonance peaks arise; their frequencies do not coincide for the wave process longitudinal and transversal components. This last leads to the fact that in one and the same elastic line, with an invariable angle of external force inclination, dependently on frequency, the longitudinal, transversal or inclined waves can propagate along the line. With it, the wave inclination does not coincide with the external force inclination, as it takes place in the lines having equal stiffness coefficients. As the examples we will consider some aspects of these models application to the geophysical problems.

Keywords: Mathematical physics; Wave physics; Theory of many-body systems; ODE systems; Dynamics; Heterogeneous dynamical systems; Elastic bended systems; Nonlinear vibration systems; Wave propagation in nonlinear media; Geophysics; Tectonics; Seismology

Classification by MSC 2000: 34A34, 34C15, 37N05, 37N15, 70E55, 70J40, 70K30, 70K40, 70K75, 74H45.

Classification by PASC 2001: 02.60.Lj; 05.45.-a; 45.05.+x; 45.10.-b; 45.20.-d; 45.20.Dd; 45.30.+s; 45.50.-j; 45.50.Jf; 46.15.-x; 46.25.Cc; 46.40.-f; 46.40.Cd; 46.40.Ff; 46.50.+a; 46.70.-p; 46.70.Lk

1. Introduction

With all importance for the practice of modelling of elastic lumped lines having one or few bends, more or less general approaches to their solution are still absent. In the literature (see, e.g., [1]-[4] etc.) we can find mainly approximate investigations of 1D elastic lines basing directly or indirectly on the matrix methods to find the characteristic frequencies. This occurs because, though “exact analytical methods are preferable in analysis, however to obtain analytical formulas for solutions of even comparably simple differential equations meets sometimes great difficulties” [5, p.10]. Furthermore, “the lumped system in which the impedances, compliances and masses can be chosen arbitrarily is quite complicated problem. It is much more complicated than the system having distributed parameters of mass, compliance, resistance. Actually, the system with lumped parameters corresponds to that distributed which can be loaded at different points by a mass and can consist of connected equal parts. So the system with lumped parameters is hardly analysable theoretically” [1, p.156]. We know analytical investigations of elastic systems having three or four hinged rods [6], when the modelling system of differential equations offers after the variables separation to find the natural frequencies directly. In more general cases the quasi-static approximations are used by the impact coefficient [1], [2], or using St. Venant principle [7], [8]. The described approaches naturally have all demerits of quasi-static approaches. The influence coefficient introduced without knowing all phase and amplitude distinctions of dynamical process at the line heterogeneities disables us to take into account correctly the phase dependencies, when summing the point deviation conditioned by the effect of all rest elastic system elements. And St. Venant principle disables us to investigate the action of far elements of the system.

The problem of bended systems has a great application. As in this paper we will present its application to geophysics, we give here the statement of this problem in tectonic and seismic processes.

The conventional model of a tectonic earthquake [9, pp.242 – 244] states that the Earth surface receives the radial push from up to 700 km deep, coming up to the surface as a longitudinal, transversal and Rayleigh waves whose different propagation velocities (9,6; 5 and 3 – 3,5 km/s respectively) cause three shake phases [10, pp.290 – 297], [11], [12]. With it the crust vertical motions cause the faults, cracks, breaks, and “the earthquakes epicentres are located along the most cracks, or these cracks are the epicentres themselves. In the table-lands the seismic phenomena are much uncommon… However the large crack along the east Madagascar shore seems coinciding with the line of often, though weak earthquakes. The same the Ethiopian Fault with its extension along the Red Sea and the Jordan Valley coincides with the earthquakes region including the seismic centres of Lebanon and the Abyssinian plateau. After Toroddsen’s data, the Island seismic regions coincide with those separated one from another by the faults. The Rhine fault depression, between Basel and Mainz, multiply encountered the earthquakes, though negligible… Sometimes the seismic motions propagate along the entire horst, while the adjoining subsided areas stay more or less stable. The longitudinal cracks of ancient mountain ranges sometimes also are the shock lines, as for example the Caledonian channel cracks in Scotland. And the cracks related to the bends of wreath-likely placed folded mountains are especially liable to the earthquakes, and this coincidence is specifically inherent in tertiary mountain ranges surrounding Asia. More often than elsewhere on the Earth the seismic motions reveal in the Japan Great Graben. Almost all Indian earthquakes are concentrated in the corners where the Himalayan Arc meets that Iranian from one side and Malay from another. Unfortunately, sufficient attention still was not given to the close dependence of the folds meeting lines with the shock lines. But this dependence is observed in the ancient folded areas; for example the epicentre of Scandinavian earthquake 23 October 1904 was located on the axis of Christiania depression, and the swarms of Foggland earthquakes were concentrated in the corner formed by the Ore mountains and Thuringian forest” [10, pp.301 – 303].

The earthquakes caused by the tangential motions of core being the most often and intensive [10, p. 303] “ are concentrated almost exceptionally in the mountain ranges that formed not so long ago… thus, almost all seismic zones… are located in the geosynclines in which they are inherent" [10, p.303]. Furthermore, "the degree of shores seismoability corresponds to the degree of steepness of their slopes" [10, p.304].

The problems of such type are usually solved as the solid body vibration problems [13], [14], [15], [16], [17]. However on the whole it is much more complex mathematical problem to take into account all features. For example, according to [18], "the solid rocks in non-disturbed state occur very seldom… Long time the builders did not pay due attention to this circumstance or even omitted it at all. Even now one can often hear the incorrect opinion that the solid rock is some integral, continued 'whole body'… Such a concept is corroborated almost nowhere in nature and is basically wrong. In the view of mechanics the rock-mass is the "many-body system" ([18]) 'similar to a dry masonry of well-adjusted stones' ([19])… With a complete natural partition…, when the rock-mass is 'run trough by cracks', and the separate bodies limited by the cracks are perfectly isolated, like the building stones in a container or in mosaic, the rock can be properly named a many-body system… If a monolith was considered a continuous medium and obeys the continuum mechanics regularities, then the few-body and many-body systems (middle-cracked and strong-cracked systems) are discontinuous, discrete mediums whose behaviour has to be determined by the regularities of discontinuous mechanics, the science not existing yet" [18, pp.14 – 15].

Table 1. The elasticity modulus values for the rock-masses determined experimentally

The rock, its type and structure	Determination technique	Stress under the load, kg/cm^2	Load direction	Modulus of elasticity, $m^3/kg/cm^2$
Granite, hard, fresh	Pressure plates	60	‖ to the bedding	400
			⊥ to the bedding	250
Molass soundstone, small-grained	Compression plates	0 – 30	‖ to the stratification	18 – 36
Soundish marl schist, small-grained			⊥ to the stratification	13 – 26
Molass soundstone, middle- and large-grained		0 - 30	‖ to the stratification	14 – 28
			⊥ to the stratification	10 – 20
Dusty stone and grey wacke (Cambrian), fine-grained	Compression box	35	‖ to the stratification	210 – 530
			⊥ to the stratification	190
Quartzite, hard, cracked	Compression plates	Up to 40	‖ to the stratification	380
			⊥ to the stratification	280
Black schist, flaggy	Compression plates	7	‖ to the stratification	190
			⊥ to the stratification	73
Low conglomerate	Compression plates	-	Horizontally	14 – 570
			Vertically	28 – 500
Mica schist, crystalline, mylonitised	Compression box	20	‖ to the stratification	70
			⊥ to the stratification	40
Argillaceous schist, Devonian, strongly squeezed	Rafts and compression box	30	In parallel	150 – 250
			Perpendicularly	90

Furthermore, when modelling the processes, the inequality of longitudinal and transversal stiffnesses of an elastic system is a matter of great importance. The Table 1 taken from [18, pp.56 – 61] shows that for the main rocks a ratio of transversal modulus of elasticity to that longitudinal is approximately 1,5 to 2. The more, we have to mark a well-known experimental fact that "one and the same material is able to behave elastically, plastically, viscously or brittlely, dependently on the nature, value and time of the load acting… If we, being guided by methodical considerations, admit (in our mind or experimentally) that these factors are constant, then we can mathematically describe the separate types of material behaviour; with it we speak about the properties of material as of its constants, though in reality they on the whole and each separately are variable" [18, p.46]. For many materials the modulus of elasticity *E* has been determined dependently on time and speed of loading… The slowly applied and long-lasting load diminishes, and the fast and short-term load increases the modulus of elasticity *E* value" [18, p.51].

Proceeding from the said, we can describe quite completely many salient features of a vibration pattern in so complicated mechanical systems, investigating 1D lumped models having a bend at some *k*th element and introducing different longitudinal and transversal stiffnesses of elastic constraints. It became possible with the appearance of the method to obtain exact analytical solutions for 1D systems having unlimited number of elastically connected bodies that gives basically other approach to the problem. The new method presented in [20] – [24] considers the elastic system not as an aggregate of vibrant elements, as conventional methods do, but describes analytically the response to the external action of the elastic line as an integral lumped system. This method works equally successfully for finite and infinite, ideal and resistant, homogeneous and heterogeneous elastic systems.

The entire complex of problems contoured above is very wide, complicated and diversiform and cannot be described in the frames of one paper. So we will concentrate our attention on the influence of a bend in an elastic line on the pattern of vibration process, supposing that when continued, this investigation offers to describe additionally a broad complex of phenomena being out of this paper's frames.

Having now exact analytical solutions for elastic lumped and distributed systems [20] – [24] obtained without any matrix methods and fully determined in reference to the studied elastic systems parameters, we gain the possibility to find exact analytical solutions also for the lines having one or more bends. The theorem proof much simplifies the finding of solutions and the analysis of vibration pattern for a wide class of elastic systems. In this paper we will consider some of the most typical examples that can be investigated in frames of the theorem validity.

2. Theorem of bend influence on the pattern of processes

To investigate elastic bended lines, let us first prove the general theorem determining the degree of bend effect on the solution pattern.

THEOREM 1. *A bend in an elastic line does not effect on the vibration pattern only in case, when the transversal and longitudinal stiffness coefficients of its constraints are equal.*

To prove this theorem, consider some elastic line (see Fig. 1) having a bend at its k th element, and let in general case the masses of all mass elements be inequal. Suppose also that in the considered elastic line some wave process described by x and y components takes place. Conveniently introduce two reference systems (x, y) and (η, ξ) describing the vibration processes before and after the bend relatively. Their direction is shown in Fig. 1.

Then the modelling system of differential equations will have the following form:
for the x-component

$$\begin{cases} \text{.....................................} ; \\ m_{(k-1)}\dfrac{d^2\Delta_{x(k-1)}}{dt^2} = s\left(\Delta_{x(k-2)} + \Delta_{xk} - 2\Delta_{x(k-1)}\right); \\ m_k\dfrac{d^2\Delta_{xk}}{dt^2} = s\left(\Delta_{x(k-1)} + \left(\Delta_{\eta(k+1)}\cos\alpha - \Delta_{\xi(k+1)}\sin\alpha\right) - 2\Delta_{xk}\right), \end{cases} \quad (1)$$

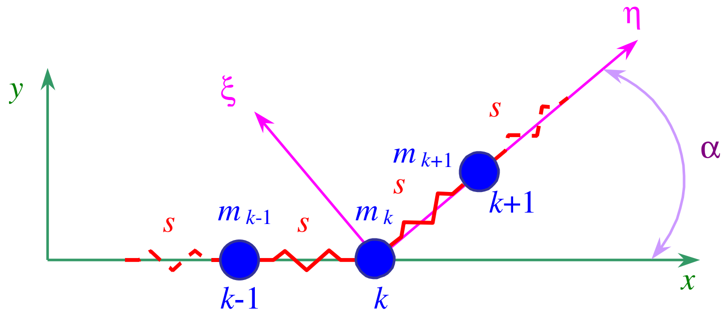

Fig. 1. The calculation scheme of an elastic line having a bend at the k th element with the angle α°

where m_k is the mass of an elastic line related element; s is the stiffness coefficient, and Δ_{xk} is the k th element displacement along the axis x;

for the η -component

$$\begin{cases} m_{(k+1)}\dfrac{d^2\Delta_{\eta(k+1)}}{dt^2} = s\left(\Delta_{\eta(k+2)} + \left(\Delta_{xk}\cos\alpha + \Delta_{yk}\sin\alpha\right) - 2\Delta_{\eta(k+1)}\right), \\ m_{(k+2)}\dfrac{d^2\Delta_{\eta(k+2)}}{dt^2} = s\left(\Delta_{\eta(k+3)} + \Delta_{\eta(k+1)} - 2\Delta_{\eta(k+2)}\right), \\ \dots\dots\dots\dots\dots\dots\dots\dots\dots\dots; \end{cases} \tag{2}$$

for the y -component

$$\begin{cases} \dots\dots\dots\dots\dots\dots\dots\dots\dots\dots, \\ m_{(k-1)}\dfrac{d^2\Delta_{y(k-1)}}{dt^2} = s\left(\Delta_{y(k-2)} + \Delta_{yk} - 2\Delta_{y(k-1)}\right), \\ m_k\dfrac{d^2\Delta_{yk}}{dt^2} = s\left(\Delta_{y(k-1)} + \left(\Delta_{\eta(k+1)}\sin\alpha + \Delta_{\xi(k+1)}\cos\alpha\right) - 2\Delta_{yk}\right); \end{cases} \tag{3}$$

for the ξ -component

$$\begin{cases} m_{(k+1)}\dfrac{d^2\Delta_{\xi(k+1)}}{dt^2} = s\left(\Delta_{\xi(k+2)} + \left(-\Delta_{xk}\sin\alpha + \Delta_{yk}\cos\alpha\right) - 2\Delta_{\xi(k+1)}\right), \\ m_{(k+2)}\dfrac{d^2\Delta_{\xi(k+2)}}{dt^2} = s\left(\Delta_{\xi(k+3)} + \Delta_{\xi(k+1)} - 2\Delta_{\xi(k+2)}\right), \\ \dots\dots\dots\dots\dots\dots\dots\dots\dots\dots\ , \end{cases} \tag{4}$$

First of all note that according to the conventional rule of co-ordinate transformation, we can substitute in (1) and (3) the parameters describing the k th mass displacement located at the bend

$$\begin{aligned} &\Delta_{\eta(k+1)}\cos\alpha - \Delta_{\xi(k+1)}\sin\alpha = \Delta_{x(k+1)} \\ &\Delta_{\eta(k+1)}\sin\alpha + \Delta_{\xi(k+1)}\cos\alpha = \Delta_{y(k+1)} \end{aligned} \tag{5}$$

The similar relation will be true for the rest line elements located after the bend. Taking this into account, multiply (2) into $\cos\alpha$, (4) into $\sin\alpha$ and subtract (4) from (2) term by term. After the manipulation we yield

$$\begin{cases} m_{(k+1)}\dfrac{d^2\Delta_{x(k+1)}}{dt^2} = s\left(\Delta_{x(k+21)} + \Delta_{xk} - 2\Delta_{x(k+1)}\right), \\ m_{(k+2)}\dfrac{d^2\Delta_{x(k+2)}}{dt^2} = s\left(\Delta_{x(k+3)} + \Delta_{x(k+1)} - 2\Delta_{x(k+2)}\right), \\ \dots\dots\dots\dots\dots\dots\dots\dots\dots\dots\dots\ . \end{cases} \tag{6}$$

Multiplying (2) into $\sin\alpha$ and (4) into $\cos\alpha$ and summing them term by term, we yield

$$\begin{cases} m_{(k+1)}\dfrac{d^2\Delta_{y(k+1)}}{dt^2} = s\left(\Delta_{y(k+21)} + \Delta_{yk} - 2\Delta_{y(k+1)}\right), \\ m_{(k+2)}\dfrac{d^2\Delta_{y(k+2)}}{dt^2} = s\left(\Delta_{y(k+3)} + \Delta_{y(k+1)} - 2\Delta_{y(k+2)}\right), \\ \dots\dots\dots\dots\dots\dots\dots\dots\dots\dots\dots\ . \end{cases} \tag{7}$$

Integrating (1), (3), (6) and (7) and noting (4), we see that the transformed system of differential equations is already independent of the angle α. Consequently, the solutions in co-ordinates (x, y) will be invariable in the view of a bend.

As opposite to this, if the longitudinal and transversal stiffnesses of an elastic line are different, then in the initial modelling systems of differential equations we have to introduce the stiffness s_{lt} in (1) and (2), and s_{tr}, $s_{tr} \neq s_{lt}$ in (3) and (4). It is easy to check that after it every attempt to transform the system (η,ξ) into (x, y) for the equations of the line elements located after the bend will not lead to such simplification. The angle α will remain in the modelling system of equations, therefore it will be present in the solutions describing the vibration process. In this case we have to consider the elastic system as that having an additional distinction at the bend point. The difference between the longitudinal and transversal stiffness values will lead to the different along-the-line wave propagation velocities, and the complicated vibration patterns will arise needing the additional studying.

The proven theorem can be easy extended to the generalised co-ordinates of an elastic system. At the same time, the definition of generalised co-ordinates per se cannot substitute the essence of the proved assertion, since, according to the theorem, the modelling system much simplifies with the equal longitudinal and transversal stiffness, and instead two systems (η,ξ) and (x, y) it can be reduced to the general system (x, y) excluding the influence of the bend angle α.

In this paper we will determine the solution for some elastic line models in whose investigation this theorem is valid and which are widely applicable to the specific problems.

3. 1D homogeneous elastic lumped system with equal longitudinal and transversal stiffness coefficients

This model can be helpful in studying the problems reduced to the infinitesimally thin rods, homogeneous, isotropic materials and so on. The typical form of the model is shown in Fig. 2. As

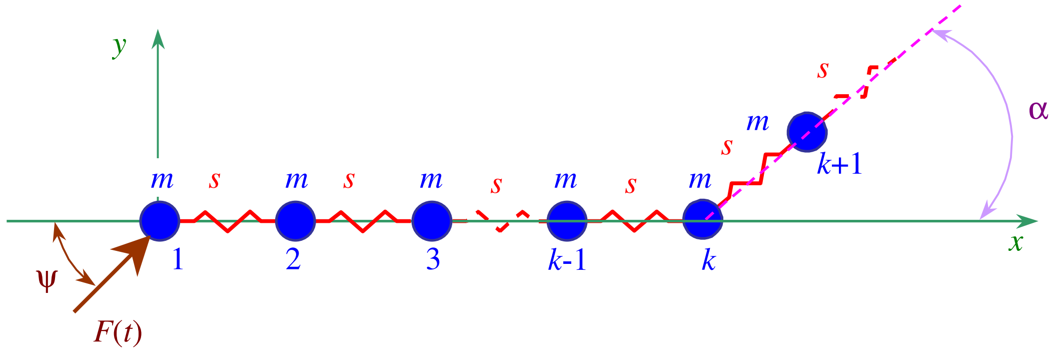

Fig. 2. The calculation scheme of 1D homogeneous elastic line having a bend at the k th element with the bend angle α° and equal coefficients of longitudinal and transversal stiffnesses

we proved in the theorem, in this case we can disregard the angle α in the modelling system of differential equations, so the system will take the following form:
for the x-component

$$\begin{cases} m\dfrac{d^2\Delta_{x1}}{dt^2} = F(t)\cos\psi - s(\Delta_{x2} - \Delta_{x1}), \\ \dots\dots\dots\dots\dots\dots\dots\dots, \\ m\dfrac{d^2\Delta_{x(k-1)}}{dt^2} = s\left(\Delta_{x(k-2)} + \Delta_{xk} - 2\Delta_{x(k-1)}\right), \\ m\dfrac{d^2\Delta_{xk}}{dt^2} = s\left(\Delta_{x(k-1)} + \Delta_{x(k+1)} - 2\Delta_{xk}\right), \\ \dots\dots\dots\dots\dots\dots\dots\dots, \end{cases} \tag{8}$$

and for the y-component

$$\begin{cases} m\dfrac{d^2\Delta_{y1}}{dt^2} = F(t)\sin\psi - s(\Delta_{y2} - \Delta_{y1}), \\ \dots\dots\dots\dots\dots\dots\dots\dots, \\ m\dfrac{d^2\Delta_{y(k-1)}}{dt^2} = s\left(\Delta_{y(k-2)} + \Delta_{yk} - 2\Delta_{y(k-1)}\right), \\ m\dfrac{d^2\Delta_{yk}}{dt^2} = s\left(\Delta_{y(k-1)} + \Delta_{y(k+1)} - 2\Delta_{yk}\right), \\ \dots\dots\dots\dots\dots\dots\dots\dots, \end{cases} \tag{9}$$

where ψ is the angle of an external force inclination to the axis x, and $F(t) = F_0 e^{j(\omega t + \varphi_0)}$ is the external force acting on the start of line.

Using the results presented in [20], we can write the solutions for (8) and (9).

At the subcritical band (periodical vibration regime) at $\omega < \omega_0$

for the x-component

$$\Delta_{xi} = -j\frac{F_0\cos\psi}{\omega\sqrt{sm}} e^{j[\omega t - (2i-1)\tau + \varphi_0]}, \tag{10}$$

for the y-component

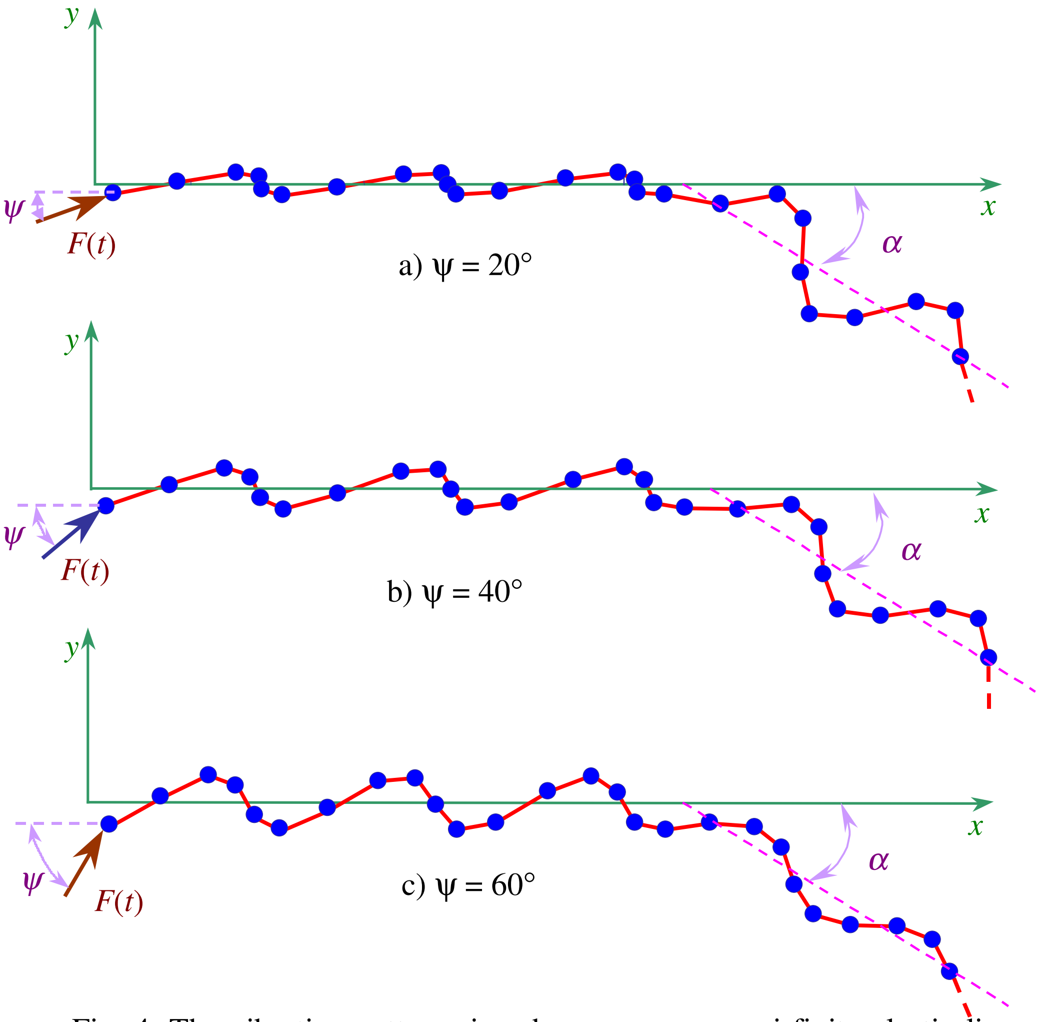

Fig. 4. The vibration patterns in a homogeneous semi-finite elastic line having a bend angle $\alpha = -32^{\circ}$ at the 17th line element, with respect to the external force inclination angle ψ to the axis x. The line parameters: $s = 100\,\text{N/m}$; $m = 0{,}01\,\text{kg}$; $F_0 = 1\,\text{N}$; $\omega = 110\,\text{sec}^{-1}$

$$\Delta_{yi} = -j\frac{F_0 \sin\psi}{\omega\sqrt{sm}}e^{j\left[\omega t-(2i-1)\tau+\varphi_0\right]}. \tag{11}$$

where $\tau = \arcsin\beta$, $\beta = \sqrt{\omega^2 m/4s}$, $i = 1, 2.3, \ldots$.

At the overcritical band (aperiodical vibration regime) at $\omega > \omega_0$

for the x-component

$$\Delta_{xi} = (-1)^i \frac{F_0 \cos\psi}{2s\beta}\gamma_-^{2i-1}e^{j(\omega t+\varphi_0)}, \tag{12}$$

for the y-component

$$\Delta_{yi} = (-1)^i \frac{F_0 \sin\psi}{2s\beta}\gamma_-^{2i-1}e^{j(\omega t+\varphi_0)}, \tag{13}$$

where $\gamma_- = \beta - \sqrt{\beta^2 - 1}$.

At the critical frequency (critical vibration regime) at $\omega = \omega_0$

for the x-component

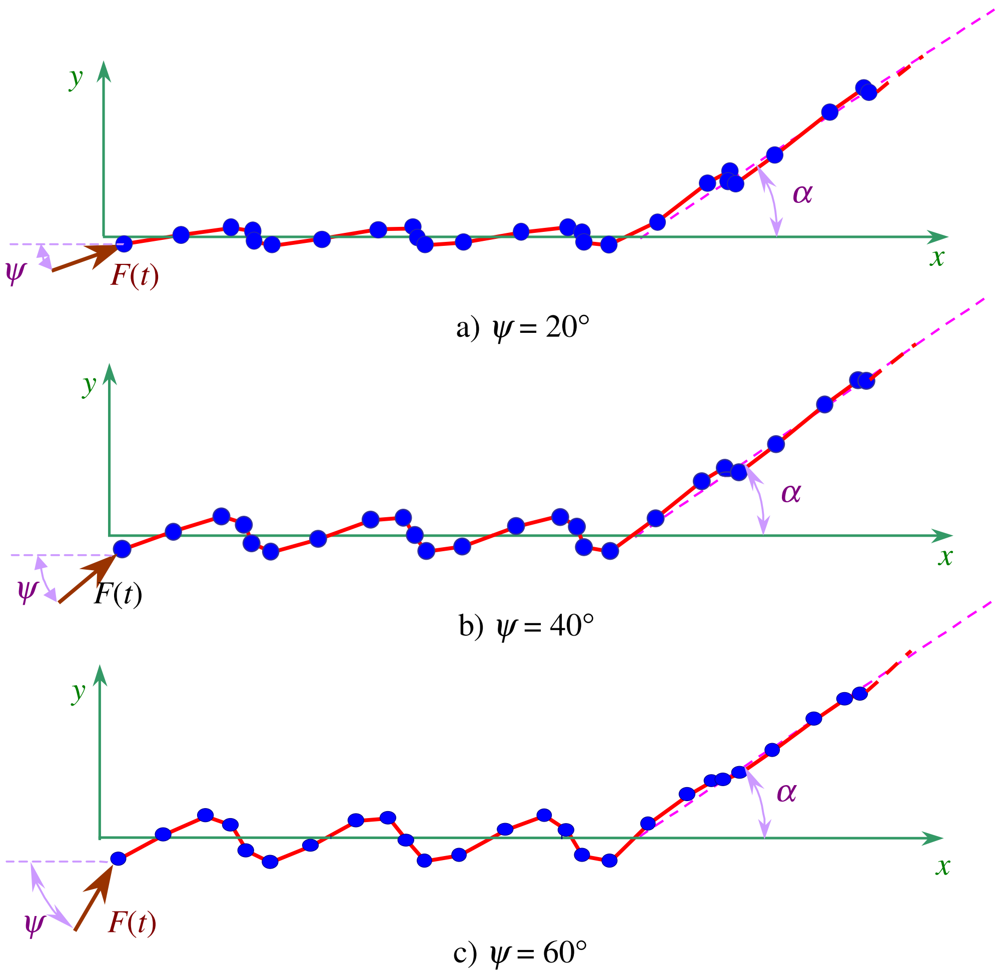

Fig. 3. The vibration patterns in a homogeneous semi-finite elastic line having a bend with angle $\alpha = 32^{\circ}$ at the 17th line element, with respect to the external force inclination angle ψ to the axis x. The line parameters: $s = 100$ N/m; $m = 0{,}01$ kg; $F_0 = 1$ N; $\omega = 110\,\text{sec}^{-1}$

$$\Delta_{xi} = (-1)^i \frac{F_0 \cos\psi}{2s} e^{j(\omega t + \varphi_0)}, \tag{14}$$

for the y-component

$$\Delta_{yi} = (-1)^i \frac{F_0 \sin\psi}{2s} e^{j(\omega t + \varphi_0)}. \tag{15}$$

As was supposed, the difference between x and y components is only the value of external force amplitude projections, and the solutions before and after the bend do not differ. None the less, the vibration patterns within the indicated regions will differ. In Fig. 3 the typical pattern is shown dependently on the external force inclination angle ψ at the positive angles α, and in Fig. 4 – at the negative α. In Fig. 5 the diagrams of typical vibrations in the lines with positive and negative bend angles are shown dependently on the external force momentary phase $\Theta = \omega t + \varphi_0$. As we can see from the construction, in the region before the bend in all the diagrams the inclined waves propagate. The inclination value equals to the angle of an external force inclination to the axis x. During the vibration process all elements move elliptically, in full correspondence with the multiple experimental facts (see e.g. [13, pp.300 – 301]). In the after-bend region, with positive α we see the decreasing amplitude of a longitudinal component, and vice versa with negative α. At the same

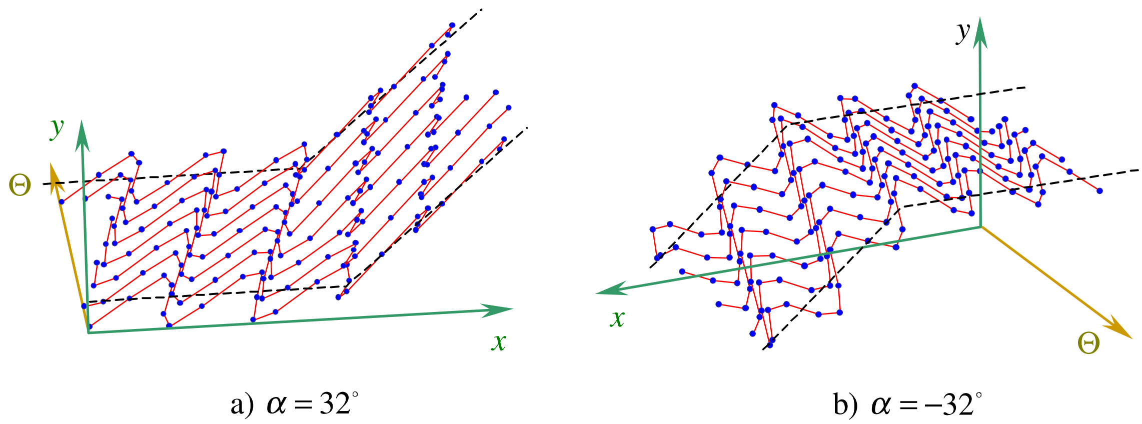

Fig. 5. The vibration patterns in a homogeneous semi-finite elastic line having the bend angle α at the 17th line element, with respect to the external force momentary phase $\Theta = \omega t + \varphi_0$ at the external force inclination angle $\psi = 40^\circ$ to the axis x. The line parameters: $s = 100$ N/m; $m = 0{,}01$ kg; $F_0 = 1$ N; $\omega = 110\,\text{sec}^{-1}$

time, with the positive α the wave front slop grows with growing ψ, and with the negative α it diminishes with growing ψ.

These transformations of the vibration pattern can be simply explained by the regularities of transformation from the (x, y) reference system to that (η, ξ).

On the basis of Fig. 1 construction, the transfer conditions between the reference systems take the form

$$\begin{aligned} \Delta_\eta &= \Delta_x \cos\alpha + \Delta_y \sin\alpha \\ \Delta_\xi &= -\Delta_x \sin\alpha + \Delta_y \cos\alpha \,. \end{aligned} \tag{16}$$

Substituting, for example, (10) and (11) into (16), we yield: or the η-component

$$\Delta_{\eta i} = -j\frac{F_0 \cos(\psi - \alpha)}{\omega\sqrt{sm}} e^{j[\omega t - (2i-1)\tau + \varphi_0]} \tag{17}$$

and for the ξ-component

$$\Delta_{\xi i} = -j\frac{F_0 \sin(\psi - \alpha)}{\omega\sqrt{sm}} e^{j[\omega t - (2i-1)\tau + \varphi_0]} \tag{18}$$

We can see from (17) and (18) that with the positive α comparable with ψ, the longitudinal η-component predominates, and with the negative α the transversal ξ-component predominates. The longitudinal component value determines the front slop. Just due to it with the positive α the front slop increases, and with that negative it diminishes.

The considered example shows that despite the bend angle effect on the solutions is absent, in the specific elastic line models their own distinctions arise that are caused by the co-ordinate systems transformation regularities before and after the bend point.

4. Closed-loop homogeneous elastic lumped system

Consider a closed-loop homogeneous line consisting of n elements connected by means of elastic linear constraints having equal transversal and longitudinal stiffnesses; its general form is presented in Fig. 6a. According to the proved theorem, this line can be presented as a linear chain whose first mass is rigidly connected with the nth elastic constraint, just as it is shown in Fig. 6b. The modelling system of differential equations for this line is following:
for the x-component

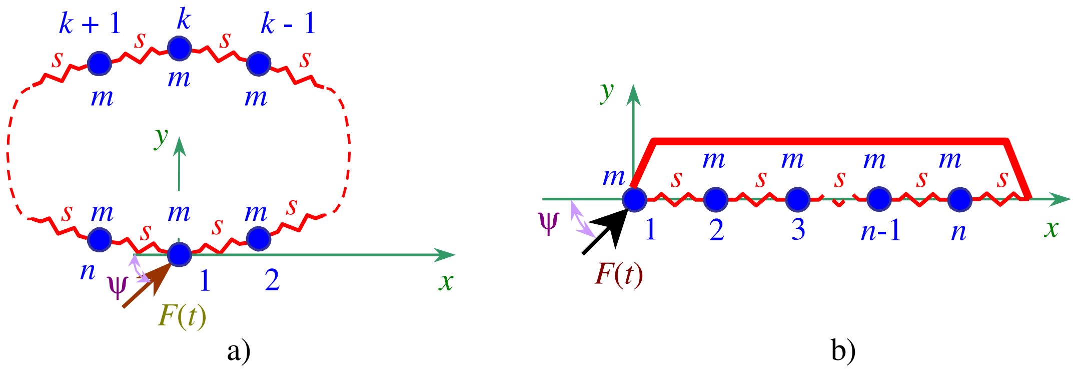

Fig. 6. The calculation scheme of a homogeneous closed-loop elastic line consisting of n elements under the harmonic force $F(t)$ acting with the angle ψ to the axis x

$$\begin{cases} m\dfrac{d^2\Delta_{x1}}{dt^2} = F(t)\cos\psi - s\left(\Delta_{xn} + \Delta_{x2} - 2\Delta_{x1}\right), \\ m\dfrac{d^2\Delta_{x2}}{dt^2} = s\left(\Delta_{x3} + \Delta_{x1} - 2\Delta_{x2}\right) \\ \dots\dots\dots\dots\dots\dots\dots\dots\dots, \\ m\dfrac{d^2\Delta_{x(n-1)}}{dt^2} = s\left(\Delta_{x(n-2)} + \Delta_{xn} - 2\Delta_{x(n-1)}\right), \\ m\dfrac{d^2\Delta_{xn}}{dt^2} = s\left(\Delta_{x1} + \Delta_{x(n-1)} - 2\Delta_{xn}\right), \end{cases} \tag{19}$$

and for the y-component

$$\begin{cases} m\dfrac{d^2\Delta_{y1}}{dt^2} = F(t)\sin\psi - s\left(\Delta_{yn} + \Delta_{y2} - 2\Delta_{y1}\right), \\ m\dfrac{d^2\Delta_{y2}}{dt^2} = s\left(\Delta_{y3} + \Delta_{y1} - 2\Delta_{y2}\right) \\ \dots\dots\dots\dots\dots\dots\dots\dots\dots, \\ m\dfrac{d^2\Delta_{y(n-1)}}{dt^2} = s\left(\Delta_{y(n-2)} + \Delta_{yn} - 2\Delta_{y(n-1)}\right), \\ m\dfrac{d^2\Delta_{yn}}{dt^2} = s\left(\Delta_{y1} + \Delta_{y(n-1)} - 2\Delta_{yn}\right). \end{cases} \tag{20}$$

As opposite to (8)-(9), the systems of modelling equations (19)-(20) are finite, and the first and last equations of the systems (19)-(20) are connected by the cross relation through the parameters Δ_{x1}, Δ_{y1} and Δ_{xn}, Δ_{yn} relatively. It certainly reflects on the solutions.

In the periodical vibration regime ($\omega < \omega_0$), within the elastic line, the standing wave will form, since the solutions have the following form:
for the x-component

$$\Delta_{xi} = -\frac{F_0\cos\psi\cos\left[n-2(i-1)\right]\tau}{2\omega\sqrt{sm}\cos\tau\sin n\tau}e^{j[\omega t+\varphi_0]};\ i = 1,2,3,\dots,n, \tag{21}$$

and for the y-component

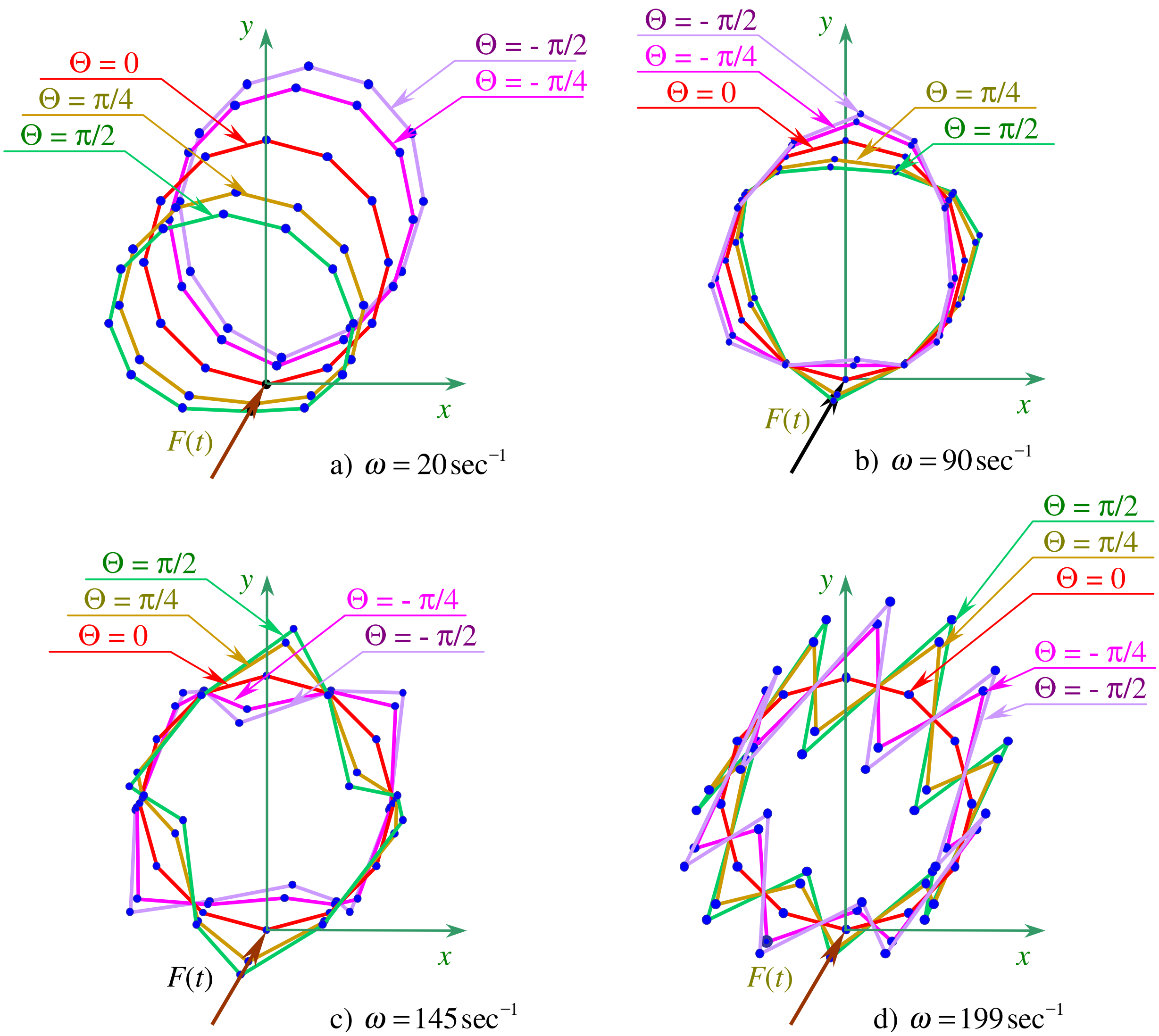

Fig. 7. The diagrams of typical vibrations in a lumped homogeneous closed-loop elastic line under the harmonic external force inclined to the axis x at the angle $\psi = 60^\circ$, with respect to the circular frequency ω and external force momentary phase $\Theta = \omega t + \varphi_0$. The elastic line parameters: $n = 12$; $a = 0,02$ m; $s = 100$ N/m; $m = 0,01$ kg; $F_0 = 1$ N; $\omega_0 = 200\,\sec^{-1}$

$$\Delta_{yi} = -\frac{F_0 \sin\psi \cos\left[n - 2(i-1)\right]\tau}{2\omega\sqrt{sm}\cos\tau \sin n\tau} e^{j[\omega t + \varphi_0]}. \tag{22}$$

In the aperiodical regime ($\omega > \omega_0$), we see the antiphase vibrations damping along the line in the region of external force action, because the solutions have the following form:
for the x-component

$$\Delta_{xi} = (-1)^i \frac{F_0 \cos\psi \left[\gamma_+^{n-2(i-1)} + (-1)^n \gamma_-^{n-2(i-1)}\right]}{2\omega\sqrt{sm\left(\beta^2 - 1\right)}\left[\gamma_+^n + (-1)^n \gamma_-^n\right]} e^{j(\omega t + \varphi_0)}, \tag{23}$$

and for the y-component

$$\Delta_{xi} = (-1)^i \frac{F_0 \sin\psi \left[\gamma_+^{n-2(i-1)} + (-1)^n \gamma_-^{n-2(i-1)}\right]}{2\omega\sqrt{sm\left(\beta^2 - 1\right)}\left[\gamma_+^n + (-1)^n \gamma_-^n\right]} e^{j(\omega t + \varphi_0)}, \tag{24}$$

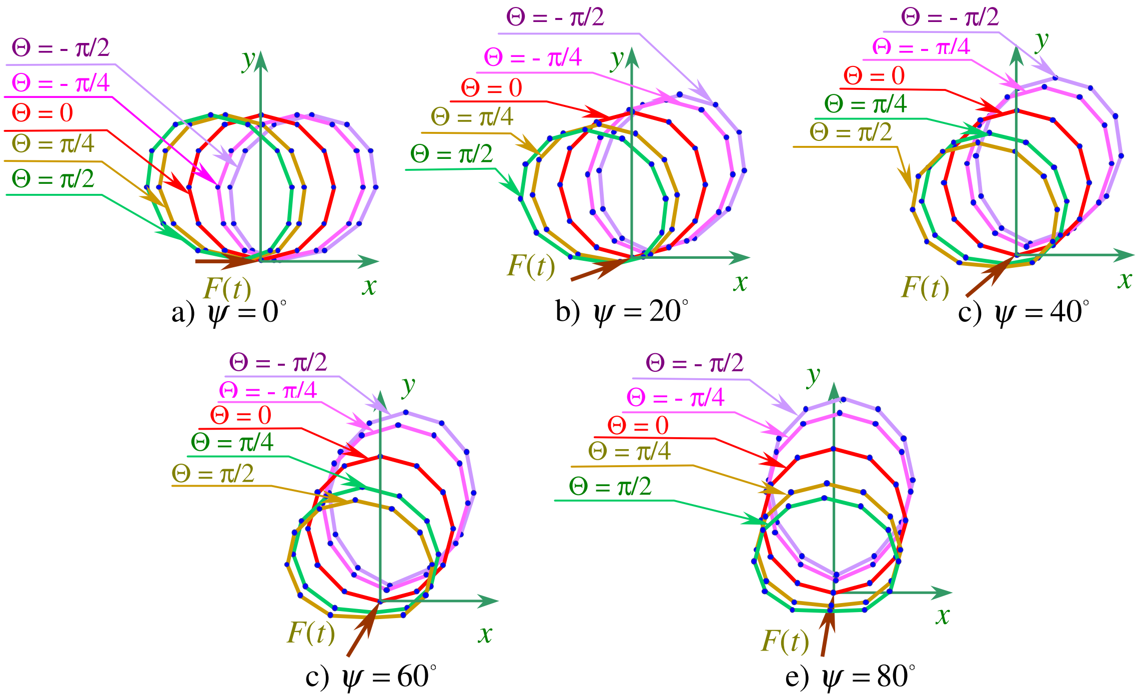

Fig. 8. The typical vibrations in a lumped homogeneous closed-loop elastic line under the harmonic external force acting with the circular frequency $\omega = 20\sec^{-1}$, with respect to the angle ψ of the external force inclination to the axis x. The line parameters: $n = 12$; $a = 0,02$ m; $s = 100$ N/m; $m = 0,01$ kg; $F_0 = 1$ N; $\omega_0 = 200\sec^{-1}$

where $\gamma_+ = \beta + \sqrt{\beta^2 - 1}$, $\gamma_- = \beta - \sqrt{\beta^2 - 1}$.

The solutions for critical regime ($\omega = \omega_0$) depend on the number n evenness. With the even n the values Δ_{xi} and Δ_{yi} are infinite, and with the odd n the solutions take the following form:

for the x-component

$$\Delta_{xi} = (-1)^i \frac{F_0 \cos\psi}{2s} e^{j(\omega t + \varphi_0)}, \tag{25}$$

and for the y-component

$$\Delta_{yi} = (-1)^i \frac{F_0 \sin\psi}{2s} e^{j(\omega t + \varphi_0)}. \tag{26}$$

It means, they practically coincide with the solutions (14)-(15).

In Figures 7 and 8, the typical diagrams are presented dependently on the external force frequency ω and its inclination angle ψ to the axis x relatively. They were constructed on the basis of above solutions for the closed-loop elastic line. We can see in Fig. 7 that actually in the line the standing waves produce, and they are in parallel to the excitation force direction. This last is easy explainable by the theorem and (22)-(26):

$$\frac{\Delta_{yi}}{\Delta_{xi}} = \tan\psi. \tag{27}$$

The construction in Fig. 8 corroborates it. It is clearly seen that with the varying external force inclination, the inclination of vibrations varies too.

Furthermore, we can see from Fig. 7 that as the frequency tends to critical, the vibration shape tends to that antiphase, and according to (23)-(24), it remains such in the aperiodical regime. The

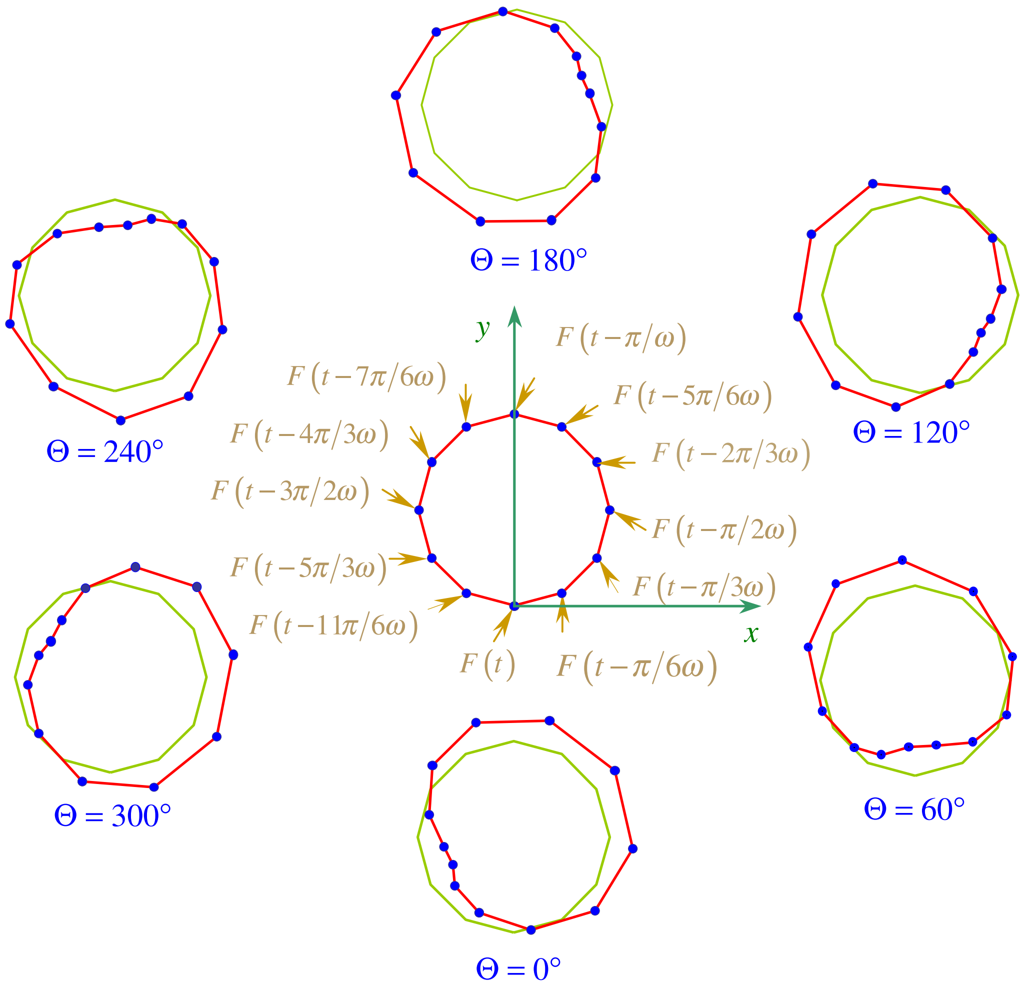

Fig. 9. The closed homogeneous elastic line vibrations under the external distributed harmonic force acting as the travelling wave with the circular frequency $\omega = 90\,\text{sec}^{-1}$ and at the angle $\psi = 60^{\circ}$, with respect to the external force momentary phase Θ. The line parameters: $n = 12$; $a = 0{,}02$ m; $s = 100$ N/m; $m = 0{,}01$ kg; $F_0 = 1$ N; $\omega_0 = 200\,\text{sec}^{-1}$

only, in the aperiodical regime there is added the along-the-line damping which localises the external excitation energy in the external force action region.

Basing on (21)-(22), we can easy obtain the solution for the case when a distributed force with the phase delay $2\pi/n$ acts on a closed-loop line. This problem is applicable to the rotary and rolling models. To solve it, it is sufficient to sum the related solutions (21)-(22) as to all the elements, taking into account the phases delay. The typical form of vibrations in such model is presented in Fig. 9. We see that unlike the above case, the travelling waves produce in the line, and the vibration pattern does not correspond to Fig. 7b. As opposite to the vibration pattern being formed in the line by a concentrated force, in this case the half-period wave process propagates in the line. And its propagation velocity is determined by the parameters of external force, not of the elastic line. With the growing frequency the vibration pattern complicates, but even when approaching to the critical frequency, the vibration pattern will not be so clearly expressed as in case of concentrated force action. We can see it well in Fig. 10, where the diagrams are presented dependently on the external force frequency.

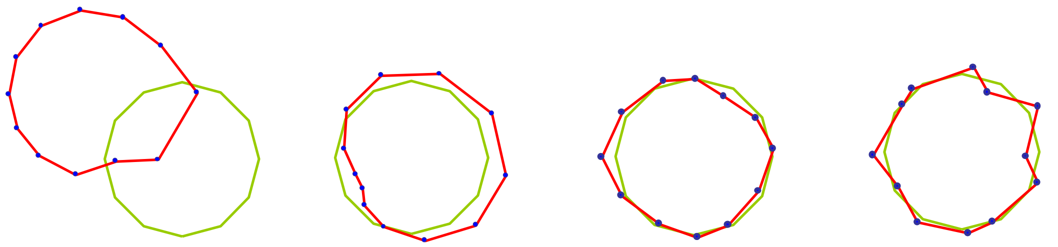

Fig. 10. The closed homogeneous elastic line vibrations under the external distributed harmonic force acting as the travelling wave at the angle $\psi = 60^\circ$ and at the moment $\Theta = 0$, with respect to the external force circular frequency ω. The line parameters: $n = 12$; $a = 0{,}02$ m; $s = 100$ N/m; $m = 0{,}01$ kg; $F_0 = 0{,}5$ N; $\omega_0 = 200\,\sec^{-1}$

Thus, on the closed-loop elastic line model we see also that despite the bend angle does not effect on the solution directly, each specific model reveals its distinctions. But they are conditioned by the distinctions of transition between the reference systems.

5. 1D homogeneous elastic line having inequal longitudinal and transversal stiffness coefficients

As we said in the introduction, the rocks with which we deal in geological and engineering problems are usually differently deformable in the longitudinal and transversal directions of a rock. So as the third example we will consider the vibration pattern variation in case of inequal longitudinal and transversal stiffness coefficients of an elastic line. In the item 2 we proved that in this case we cannot ignore the bend. Two parameters characterise now the constraints stiffness – the longitudinal s_{lt} and transversal s_{tr} stiffness coefficients. The modelling systems of equations for the semi-finite homogeneous elastic line takes the following form:
for the longitudinal component

$$\begin{cases} m\dfrac{d^2\Delta_{x1}}{dt^2} = F(t)\cos\psi - s_{lt}\left(\Delta_{x2} - \Delta_{x1}\right), \\ \dots\dots\dots\dots\dots\dots\dots\dots, \\ m\dfrac{d^2\Delta_{x(k-1)}}{dt^2} = s_{lt}\left(\Delta_{x(k-2)} + \Delta_{xk} - 2\Delta_{x(k-1)}\right), \\ m\dfrac{d^2\Delta_{xk}}{dt^2} = s_{lt}\left(\Delta_{x(k-1)} + \left(\Delta_{\eta(k+1)}\cos\alpha - \dfrac{s_{tr}}{s_{lt}}\Delta_{\xi(k+1)}\sin\alpha\right) - 2\Delta_{xk}\right), \\ m\dfrac{d^2\Delta_{\eta(k+1)}}{dt^2} = s_{lt}\left(\Delta_{\eta(k+2)} + \left(\Delta_{xk}\cos\alpha + \dfrac{s_{tr}}{s_{lt}}\Delta_{yk}\sin\alpha\right) - 2\Delta_{\eta(k+1)}\right), \\ m\dfrac{d^2\Delta_{\eta(k+2)}}{dt^2} = s_{lt}\left(\Delta_{\eta(k+3)} + \Delta_{\eta(k+1)} - 2\Delta_{\eta(k+2)}\right), \\ \dots\dots\dots\dots\dots\dots\dots\dots\ , \end{cases} \tag{28}$$

and for the transversal component

$$\begin{cases} m\dfrac{d^2\Delta_{y1}}{dt^2} = F(t)\sin\psi - s_{tr}\left(\Delta_{y2} - \Delta_{y1}\right), \\ \ldots\ldots\ldots\ldots\ldots\ldots\ldots\ldots\ldots\ldots\ldots, \\ m\dfrac{d^2\Delta_{y(k-1)}}{dt^2} = s_{tr}\left(\Delta_{y(k-2)} + \Delta_{yk} - 2\Delta_{y(k-1)}\right), \\ m\dfrac{d^2\Delta_{yk}}{dt^2} = s_{tr}\left(\Delta_{y(k-1)} + \left(\dfrac{s_{lt}}{s_{tr}}\Delta_{\eta(k+1)}\sin\alpha + \Delta_{\xi(k+1)}\cos\alpha\right) - 2\Delta_{yk}\right), \\ m\dfrac{d^2\Delta_{\xi(k+1)}}{dt^2} = s_{tr}\left(\Delta_{\xi(k+2)} + \left(-\dfrac{s_{lt}}{s_{tr}}\Delta_{xk}\sin\alpha + \Delta_{yk}\cos\alpha\right) - 2\Delta_{\xi(k+1)}\right), \\ m\dfrac{d^2\Delta_{\xi(k+2)}}{dt^2} = s_{tr}\left(\Delta_{\xi(k+3)} + \Delta_{\xi(k+1)} - 2\Delta_{\xi(k+2)}\right), \\ \ldots\ldots\ldots\ldots\ldots\ldots\ldots\ldots\ldots\ldots\ldots\ . \end{cases} \tag{29}$$

The systems (28)-(29) differ from (1)-(4) by the k th and $(k+1)$ th equations of the modelling systems. The displacements of transient line elements Δx_k, Δy_k, $\Delta\eta_{k+1}$, $\Delta\xi_{k+1}$ are included to (28)-(29) with the coefficient

$$\zeta = \frac{s_{tr}}{s_{lt}}, \tag{30}$$

which does not offer us to transform the co-ordinates (η,ξ) into (x,y), as in case of equal stiffness coefficients. With it the solution considerably complicates. First of all, there arise two parameters

$$\tau_{lt} = \arcsin\sqrt{\frac{\omega^2 m}{4s_{lt}}} \quad \text{and} \quad \tau_{tr} = \arcsin\sqrt{\frac{\omega^2 m}{4s_{tr}}}, \tag{31}$$

characterising the delay of along-the-line propagation of the wave longitudinal and transversal components, and in general case these parameters differ. In this connection, the critical frequencies for the longitudinal and transversal components are also different and equal to

$$\omega_{lt} = 2\sqrt{\frac{s_{lt}}{m}} \quad \text{and} \quad \omega_{tr} = 2\sqrt{\frac{s_{tr}}{m}} \tag{32}$$

relatively. It causes the division of the frequency range not into two but into tree sections. In that first the vibrations of both longitudinal and transversal components relate to the periodical vibration regime. With the typical relationship of stiffnesses

$$\zeta > 1 \tag{33}$$

this band has the bounds $0 \le \omega < \omega_{lt}$. In the second band $\omega_{lt} < \omega < \omega_{tr}$, when (33) was true, the longitudinal component vibrations relate to the critical regime of antiphase along-the-line damping vibrations, and for the transversal component the periodical regime is typical. It causes the fact that out of external force action region and the bend, mainly transversal vibrations take place. Finally, at $\omega > \omega_{tr}$ the vibrations are observed only in the region of an external force action, since in this band the aperiodical vibration regime corresponds to the transversal component.

As we can see from the preliminary analysis, the vibration pattern essentially transforms in case of inequal stiffness coefficients. Each of three regions has its salient features that require their broad investigation. Regarding the low-frequency pattern of geophysical vibrations, in this work we will limit our investigation by the first region.

If the condition (33) was true, then in the band $0 \le \omega < \omega_{lt}$ the general solution for a semi-finite homogeneous elastic lumped line takes the following form:
for $i \le k$

$$\Delta x_i = -\frac{F_0 e^{j(\omega t+\varphi_0)}}{C\omega\sqrt{ms_{lt}}\sin 2k\tau_{lt}}\left\{C\cos\psi\cos\left[2(k-i)+1\right]\tau_{lt} + P_x\cos(2i-1)\tau_{lt}\right\},$$
$$\Delta y_i = -\frac{F_0 e^{j(\omega t+\varphi_0)}}{C\omega\sqrt{ms_{tr}}\sin 2k\tau_{tr}}\left\{C\sin\psi\cos\left[2(k-i)+1\right]\tau_{tr} + P_y\cos(2i-1)\tau_{tr}\right\}, \tag{34}$$

and for $i > k$

$$\Delta\eta_i = -j\frac{F_0 P_\eta}{C\omega\sqrt{ms_{lt}}} e^{j\{\omega t - [2(i-k)-1]\tau_{lt}+\varphi_0\}},$$
$$\Delta\xi_i = -j\frac{F_0 P_\xi}{C\omega\sqrt{ms_{tr}}} e^{-j\{\omega t - [2(i-k)-1]\tau_{tr}+\varphi_0\}}, \tag{35}$$

where

$$P_x = A\sin\alpha\cos\alpha\left(e^{-j2\tau_{lt}} - e^{-j2\tau_{tr}}\right) + B\left(\cos^2\alpha\, e^{-j2\tau_{lt}} + \sin^2\alpha\, e^{-j2\tau_{tr}} - 1\right),$$
$$P_y = A\left(\sin^2\alpha\, e^{-j2\tau_{lt}} + \cos^2\alpha\, e^{-j2\tau_{tr}} - 1\right) + B\sin\alpha\cos\alpha\left(e^{-j2\tau_{lt}} - e^{-j2\tau_{tr}}\right),$$
$$P_\eta = \left(A\sin\alpha + B\cos\alpha\right)\left(1 - e^{-j2\tau_{lt}}\right),$$
$$P_\xi = \left(A\cos\alpha - B\sin\alpha\right)\left(1 - e^{-j2\tau_{tr}}\right), \tag{36}$$

$$A = \cos\tau_{tr}\sin\psi\left[\cos(2k+1)\tau_{lt} - \left(\cos^2\alpha\, e^{-j2\tau_{lt}} + \sin^2\alpha\, e^{-j2\tau_{tr}}\right)\cos(2k-1)\tau_{lt}\right] +$$
$$+\cos\tau_{lt}\cos\psi\left\{e^{-j2\tau_{lt}} - e^{-j2\tau_{tr}}\right\}\sin\alpha\cos\alpha\cos(2k-1)\tau_{tr},$$
$$B = \cos\tau_{lt}\cos\psi\left[\cos(2k+1)\tau_{tr} - \left(\sin^2\alpha\, e^{-j2\tau_{lt}} + \cos^2\alpha\, e^{-j2\tau_{tr}}\right)\cos(2k-1)\tau_{tr}\right] +$$
$$+\cos\tau_{tr}\sin\psi\left\{e^{-j2\tau_{lt}} - e^{-j2\tau_{tr}}\right\}\sin\alpha\cos\alpha\cos(2k-1)\tau_{lt}, \tag{37}$$
$$C = \cos(2k+1)\tau_{lt}\cos(2k+1)\tau_{tr} + \cos(2k-1)\tau_{lt}\cos(2k-1)\tau_{tr} e^{-j2(\tau_{lt}+\tau_{tr})} -$$
$$-\cos(2k-1)\tau_{lt}\cos(2k+1)\tau_{tr}\left(\cos^2\alpha\, e^{-j2\tau_{lt}} + \sin^2\alpha\, e^{-j2\tau_{tr}}\right) -$$
$$-\cos(2k+1)\tau_{lt}\cos(2k-1)\tau_{tr}\left(\sin^2\alpha\, e^{-j2\tau_{lt}} + \cos^2\alpha\, e^{-j2\tau_{tr}}\right).$$

As P_x, P_y, P_η, P_ξ depend only on the elastic line parameters but do not depend on time and index i, basing on (34)-(35), we can state that with the inequal longitudinal and transversal stiffness coefficients in the before-bend region, the superposition of standing and progressive waves forms, depending not only on the line parameters but on the vibration frequency. With it, the longitudinal vibrations can produce in a line also under the transversal external force, and those transversal – also under the longitudinal external force, which is basically impossible in case of equal stiffness coefficients.

In the after-bend region the progressive wave forms; its amplitude depends not only on the line parameters and the bend angle, but on vibration frequency too. As we said above, with it the phase delay for longitudinal and transversal components differ, and this complicates the resulting pattern of the vibration process. Particularly, in the region of in-phase total phase delays we see the positive inclination of a progressive wave (i.e., the wave propagates with the angle ahead). With the antiphase total phase delay we see the negative inclination of a wave (i.e., the wave propagates with the angle back). These regions take turns.

In Fig. 11 one of typical patterns of vibration process is shown for the positive and negative bend angles α dependently on the external force action direction. It is visual in it that with quite small before-the-bend vibration amplitudes, in the bend region there forms a complicated vibration process with the inflections (Fig. 11 b, c), with breaking of the wave process continuity being generally different for the positive and negative bend angles and relating geologically to the charriages, and when excess of the rock strength – to the faults. The wave process amplitude depends essentially on the external excitation frequency and the bend angle. Particularly, in complete correspondence to Haug's description given in the introduction, the steeper the mountain range inflects and the closer to the normal the front of coming seismic wave is, the faster amplitude grows when transiting through the bend. In Fig. 12 we see the amplitude-frequency characteristic of the longitudinal and transversal components of the wave in an elastic line before the bend, with respect to ζ. At $\zeta = 1$ (the nearest curve in the plot) the amplitude-frequency characteristic has a hyperbolic form usual for ideal lines. With growing ζ the resonance peaks arise in the plots; their amplitude grows with growing ζ which can cause the local destructions on the quite stable general background. Some peaks in the middle band arise only at large values ζ; with growing ζ some peaks amplitude first grows, then smoothes. The transversal component peaks become displaced with growing ζ. This is caused by growing ω_{tr} according to (32). It is typical that despite the ideal pattern of elastic constraints the resonance peaks amplitudes are finite. The peaks location for the longitudinal and transversal components do not coincide too. In this connection, in such lines dependently on frequency either longitudinal or transversal vibrations can prevail. Thus, in the propagation of a wave having complex and especially continuous spectrum typical for solitary seismic waves, the essential transformation of the wave shape takes place. A number of frequencies are quenched in the wave travelling, and at the number of frequencies corresponding to the resonance peaks the vibration amplitude abruptly increases; this process is not synchronous for the longitudinal and transversal components. The smearing of the wave packet caused by dependence of the phase delay (of the propagation velocity in that number) on frequency adds to this. And taking into account that in the before-bend region a complex superposition of standing and progressive waves takes place, the velocity dispersion nonlinearly depends on the external excitation frequency.

For the amplitude-frequency characteristic with respect to the bend angle of an elastic line, we observe the similar pattern whose plots for the longitudinal and transversal components in the before-bend region are shown in Fig. 13. With $\alpha = 0$ (the curve in the middle part of the diagram) the amplitude-frequency characteristic has a standard for an ideal line hyperbolic form even with $\zeta > 1$. With growing α on the amplitude-frequency characteristic there arise the resonance peaks whose amplitude increases with growing α, and their pattern depends not only on the value but also on the sign of α. As applied to the seismic processes, it means that the abrupter transition from the flat country to the mountains is, and the abrupter the curvature of a mountain arc is (the Pamir knot is a typical example), the more destructive the earthquake consequences are. The same as in Fig. 12, the velocity of amplitude growing is different for different peaks. Some peaks reveal only at large values α, with growing α the low-frequency peak in Fig. 13 b coalesces with the next resonance peak, and the peaks location on the amplitude-frequency characteristic of the longitudinal and transversal components does not coincide.

With $s_{tr} \to s_{lt}$ the solutions (34)-(35) transform to those described in previous item, as we see in Figures 12 and 13 and can easy show mathematically. Actually, with equal stiffness coefficients (37) transform as follows:

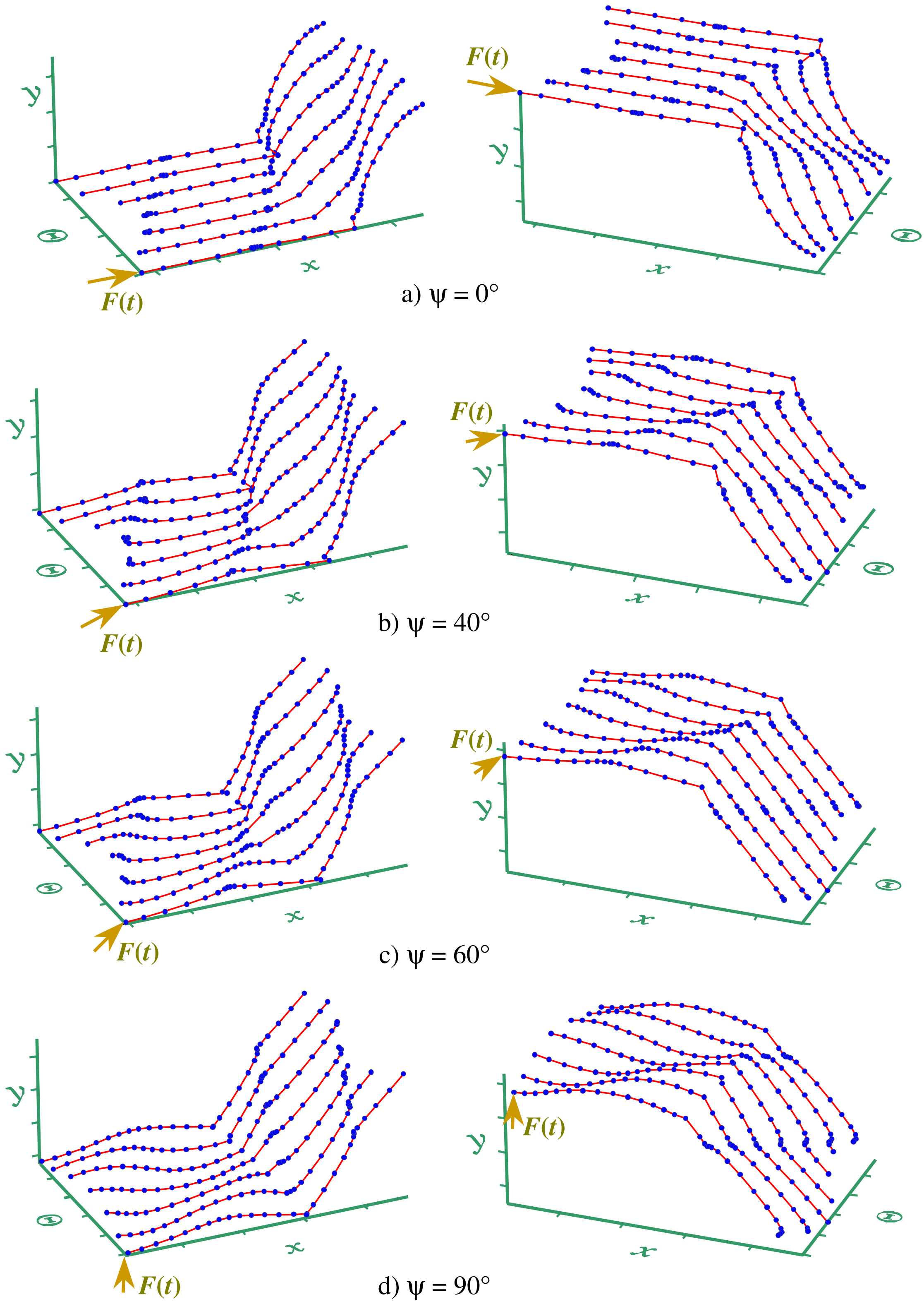

Fig. 11. The typical diagrams of vibrations in a homogeneous elastic 1D lumped system with respect to the external force momentary phase Θ and external force inclination angle ψ to the axis x, with the bend angle α equal to 60° and -60° and with the ratio of transversal stiffness to that longitudinal equal to 2,5.

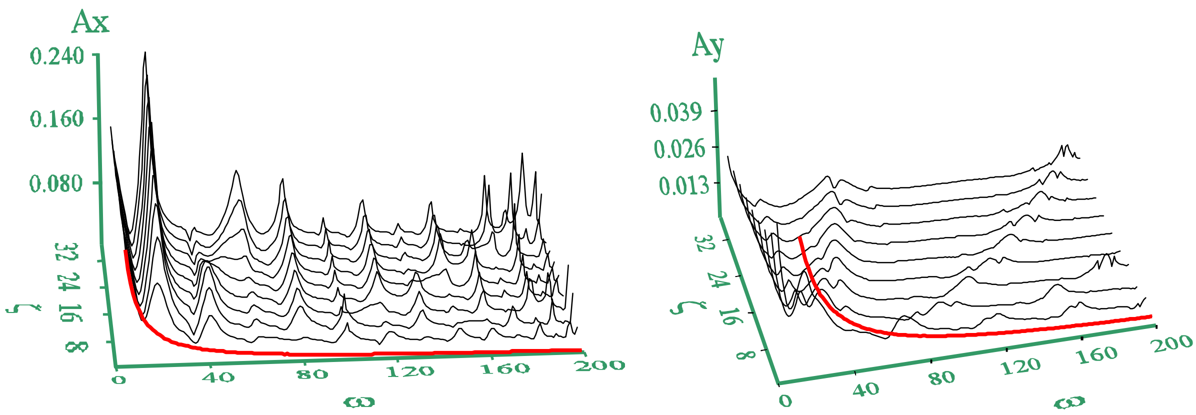

Fig. 12. The amplitude-frequency characteristic of the longitudinal (a) and transversal (b) components of vibrations in an elastic line having the bend angle $\alpha = 60^\circ$, with respect to the ratio ζ of the transversal and longitudinal stiffness coefficients. The model parameters: $m = 0{,}01$ kg , $F_0 = 1$ N , $k = 15$, $s_{lt} = 100$ N/m , $\zeta = 1{,}0 - 37{,}0$, $\psi = 45^\circ$

$$
\begin{aligned}
&A = \cos\tau \sin\psi \sin 2\tau e^{j(2k-1)\tau}, \\
&B = \cos\tau \cos\psi \sin 2\tau\, e^{j(2k-1)\tau}, \qquad (38) \\
&C = -\sin^2 2\tau\, e^{j2(2k-1)\tau},
\end{aligned}
$$

where $\tau_{lt} = \tau_{tr} = \tau$. Substituting (38) sequentially to (36) and then to (34)-(35), we obtain (10), (11), (17) and (18). For example, for Δx_i:

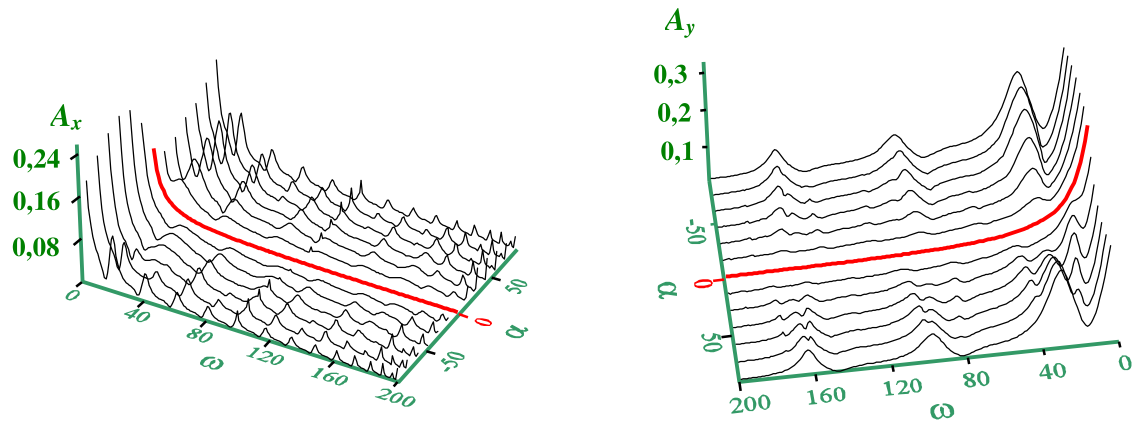

Fig. 13. The amplitude-frequency characteristic of the longitudinal (a) and transversal (b) components of vibrations in a line having different longitudinal and transversal stiffness coefficients with respect to the bend angle α. The model parameters: $m = 0{,}01$ kg , $F_0 = 1$ N , $k = 15$, $s_{lt} = 100$ N/m , $\zeta = 10$, $\psi = 45^\circ$

$$\begin{aligned}\Delta x_i &= -\frac{F_0 \cos\psi\, e^{j(\omega t+\varphi_0)}}{\omega\sqrt{ms}\sin 2k\tau}\left\{\cos\left[2(k-i)+1\right]\tau + \cos(2i-1)\tau\, e^{-j2k\tau}\right\} = \\ &= -\frac{F_0 \cos\psi\, e^{j(\omega t+\varphi_0)}}{\omega\sqrt{ms}\sin 2k\tau}\left[e^{j[2(k-i)+1]\tau} - e^{-j[2(k-i)-1]\tau}\right] = \\ &= -j\frac{F_0\cos\psi}{\omega\sqrt{sm}} e^{j[\omega t-(2i-1)\tau+\varphi_0]}.\end{aligned} \tag{39}$$

For the rest solutions of (34)-(35) the reduction is similar.

Thus we see that in case of inequal longitudinal and transversal stiffness coefficients, the vibration pattern essentially changes. In the bend region the amplitude increases, and the external force to which the table-land part of a landscape responded elastically is able to cause the folding and even destruction on the mountain slope. The same, the mountain range sections before and after its bending can respond to the seismic wave very different.

The presented diagrams show that with the further development of this subject we can gain the possibility to judge by the rocks deformation of the phenomenon which caused it, not only qualitatively but to approach to the quantitative estimations. Besides, the rock behaviour under high-frequency excitation is also interesting, when the longitudinal component vibration relates to the aperiodical regime. As we said before, in this case the wave process longitudinal component reveals only in the regions of an external force action and of the bend. In the second case it will cause the rocks destruction only in the bend region, since, as is known, the most destruction takes place namely under joint action of longitudinal and transversal components of a wave.

6. Conclusions

We have proved that the bend angle influence on the vibration pattern in an elastic line reveals only if the longitudinal and transversal stiffnesses of an elastic line are inequal. Basing on the proved theorem, we have presented the solutions for a semi-finite elastic line having a bend at the k th element in cases of equal and inequal longitudinal and transversal stiffness coefficients and for a closed-loop elastic line. We have shown that for a semi-finite line the wave front inclination changes when transiting through the bend, and this change is proportional to the bend angle. This dependency is conditioned by the transfer regularities between the reference systems.

In a closed-loop elastic line under the concentrated force action, the standing waves arises. The line elements vibration direction coincides with the external force direction. When the distributed travelling-wave-like load acted on a closed-loop line, the vibration phase delays from the external force phase. With the growing frequency, the line elements vibration pattern acquires a complicated pattern. At all frequencies the pattern differs from the case of a concentrated force action.

With inequal stiffness coefficients, in the before-bend region the superposition of standing and progressive waves takes place and the finite resonance peaks arise; their amplitude depends on the relationship between the transversal and longitudinal stiffness coefficients, on the bend angle and on the external force inclination. The resonance frequencies for the longitudinal and transversal components do not coincide. In this connection, the progressive wave inclination does not correspond to the external force inclination, as in case of equal stiffness coefficients. With the retaining given parameters and external force inclination, as longitudinal as transversal as inclined waves can propagate in the line, dependently only on the external excitation frequency. When the bend angle vanishes, the resonance peaks disappear, and two waves propagate in the line, each having the velocity proportional to the related stiffness coefficient.

The revealed features cause the bend region in a line with inequal stiffness coefficients to be a stress concentrator. In this region the vibration amplitude abruptly increases, in the vibration pattern there arise the dynamical breakdowns able to cause the additional destruction. Due to different wave propagation velocity of longitudinal and transversal components, the wave inclination is inconstant along the line. In one and the same line at one and the same moment we can observe the waves with both positive and negative inclination angles.

References:

1. Skudrzyk, E. *Simple and complex vibratory systems*. Mir, Moscow, 1971, 557 pp. (Russian, from edition: Skudrzyk E. *Simple and complex vibratory systems*. The Pennsylvania State University Press, University Park and London, 1968)

2. King N. Tong. *Theory of mechanical vibration*. State Scientific and Technical Publishing for Machinery Literature, Moscow, 1963, 354 pp. (Russian, from edition: King N. Tong. *Theory of mechanical vibration*. John Wiley & Sons, New York – London, 1961)

3. Atkinson, F.V. *Discrete and continuous boundary problems*. Mir, Moscow, 1969, 750 pp. (Russian, from edition: Atkinson F.V. *Discrete and continuous boundary problems*. Academic Press, New York – London, 1964)

4. Mirolyubov, A.A. and Soldatov, M.A. *Linear heterogeneous difference equations*. Nauka, Moscow, 1986, 126 pp. (Russian)

5. Cherepennikov, V.B. *Functional parameter method in ordinary differential equations theory*. Nauka, Suburb Division, Novosibirsk, 1983, 113 pp. (Russian)

6. Chernousko, F.L. *Snake-like motions of multibody systems over a rough plane*. Control of Oscillations and Chaos 2000. 2nd International conference, Proceedings, vol.2, pp. 321-326

7. Gonzaga Velez, P., Gimena Ramos, F.N. *Diseno de estructuras lineales*. Colleccion: Ingenieria, 1. Universidad Publica de Navarra, 1998, 184 pp. (Spanish)

8. Gimena Ramos, F. *Resolucion numerica de sistemas de ecuaciones lineales. Problemas de contorno*. Revista de edificacion RE, # 20, pp. 34-36 (Spanish)

9. Pavlinov, V.N., Kizelvater, D.S. and Lin, N.G. *Fundamentals of geology*. Nedra, Moscow, 2001, 270 pp. (Russian)

10. Haug, E. *Geology*. ONTGIZ NKTP USSR, Moscow, 1935, 576 pp. (Russian, from edition: Haug, E. *Traite de geologie*. Vol. 1. Les phenomenes geologiques. Paris, Librarie Armand Colin)

11. Savarenskiy, E.F. *Earthquakes*. In *Physical encyclopaedia*, vol.2, the cited pp.70-71. Sovetskaya encyclopedia, Moscow, 1962, 608 pp. (Russian)

12. Savarenskiy, E.F. *Seismic waves*. In: *Physical encyclopaedia*, **4**, the cited pp.507-508. Sovetskaya encyclopedia, Moscow, 1965, 592 pp. (Russian)

13. Kolski, G. *Stress waves in solids*. Inostrannaya literatura, Moscow, 1955, 200 pp. (Russian, translated from English)

14. Pfeiffer, P. *Vibrations of elastic bodies*. The All-the-Union Scientific and Technical Publishing, Moscow – Leningrad, 1934 (Russian; from edition: *Handbuch Der Physik*, band VI. Mechanik Der Elastischen Korper. Redigiert von R. Grammel. Berlin, 1928).

15. Sobolev, S.L. *Sur le vibrations d'un demiplan et d'une couche a conditions initiales arbitraire*. Mathematical collection, **40** (1933)

16. Stoneley, R. Proc. Roy. Soc. A, **103** (1924), 416

17. Love, A.E.H. *Some problems of geodynamics*. Cambridge, 1911

18. Muller, L. *Engineering geology. The rocks-mass mechanics*. Mir, Moscow, 1971, 255 pp. (Russian, from edition: Muller, L. *Der Felsbau*. Erster Band, Theoretischer Teel, Ferdinand Enke Verlag, Stuttgart, 1963)

19. Stini, J. *Technische Gesteinskunde*. Springer, Wien, 1929

20. Karavashkin, S.B. *Exact analytical solution on infinite one-dimensional elastic lumped-parameters line vibration*. Materials, Technologies, Tools. The Journal of National Academy of Sciences of Belarus, v.4, 1999, #3, pp.15-23 (Russian)

21. Karavashkin, S.B. *Exact analytical solution for 1D elastic homogeneous finite lumped line vibration.* The primted version: Materials, Technologies, Tools. The Journal of National Academy of Sciences of Belarus, **4** (1999), 4, 5-14 (Russian). The electronic version in English: SELF archive, http://angelfire.lycos.com/la3/selftrans or Mathematical Physics Preprint Archive, http://www.ma.utexas.edu/mp_arc/c/02/02-79.ps.gz

22. Karavashkin, S.B. *Some features of the forced vibrations modelling for 1D homogeneous elastic lumped lines.* The printed version: Materials, Technologies, Tools. The Journal of National Academy of Sciences of Belarus, **5** (2000), 3, 14-19 (Russian). The electronic version in English: SELF Transactions, http://angelfire.lycos.com/la3/selftrans or Mathematical Physics Preprint Archive, http://www.ma.utexas.edu/mp_arc/c/02/02-89.ps.gz

23. Karavashkin, S.B. *Peculiarities of inclined force action upon one-dimensional homogeneous elastic lumped line* arXiv, Los Alamos, USA, # math-ph/0006028

24. Karavashkin, S.B. and Karavashkina, O.N. *On complex resonance systems vibration*. SELF Transactions, http://angelfire.lycos.com/la3/selftrans or Mathematical Physics Preprint Archive, http://www.ma.utexas.edu/mp_arc/c/02/02-64.ps.gz

25. Pohl, R.V. *Mechanics, acoustics and heat theory*. The State Publishing of Technical and Theoretical Literature, Moscow, 1957, 484 pp. (Russian)